

S-AA-M-31
Cryogenic Target Handling System
Operations Manual
Volume IV—CTHS Description
Chapter 2: Target Fabrication

Table of Contents

2.1	INTRODUCTION	1
2.1.1	Glass and Polymer	2
2.1.2	Foam Targets	3
2.1.3	Coatings	3
2.1.4	Surface Finish	4
2.1.5	Low-Mass Target Mounts	4
2.2	CAPSULES FOR CRYOGENIC TARGETS	5
2.2.1	Polyimide and Glow Discharge Polymer (GDP) Fabrication ...	6
2.2.1.1	Target Burst and Buckle Parameters	8
2.2.1.2	Permeability	8
2.3	TARGET MOUNTING	10
2.3.1	Spider Silk	12
2.3.2	Spider-Silk Tensile Strength	12
2.3.3	Mechanical Properties of Silk	13
2.4	PLANAR CRYOGENIC TARGETS	13
2.5	QUALITY ASSURANCE	17
2.5.1	Silk and Mount Resonance	18

Chapter 2 Target Fabrication

2.1 INTRODUCTION

The majority of targets that are shot on OMEGA are fabricated and assembled at LLE. Capsules and some components for targets are provided by other organizations as part of the overall National Inertial Confinement Fusion Program. The LLE Target Fabrication Facility is used to fabricate, assemble, and characterize a wide assortment of targets for varying experimental campaigns. Physical and analytical methods for their preparation, inspection, and mounting have been developed.

The ICF experiments involve variations of spherical targets and planar targets. The range of target types used on OMEGA includes

- Spherical implosion targets consisting of glass or polymer shells filled with a mixture of gases;
- Surrogate targets (equivalent-sized solid spheres) used for beam pointing and focusing using the continuous UV alignment laser;
- Gold-coated spheres that are shot to provide x-ray images used to verify beam pointing and focusing;
- Planar targets used for hydrodynamic stability, equation-of-state, and plasma physics research; and
- “Hohlraum” targets for indirect-drive experiments.

LLE targets are grouped into two main classes: spherical and planar (see Fig. 2.1-1). These two categories are subdivided into room-temperature or cryo targets. A spherical cryogenic target is filled with DD or DT at pressures over 1000 atm, then cooled to 18.7°K, and layered by a differential heating method.

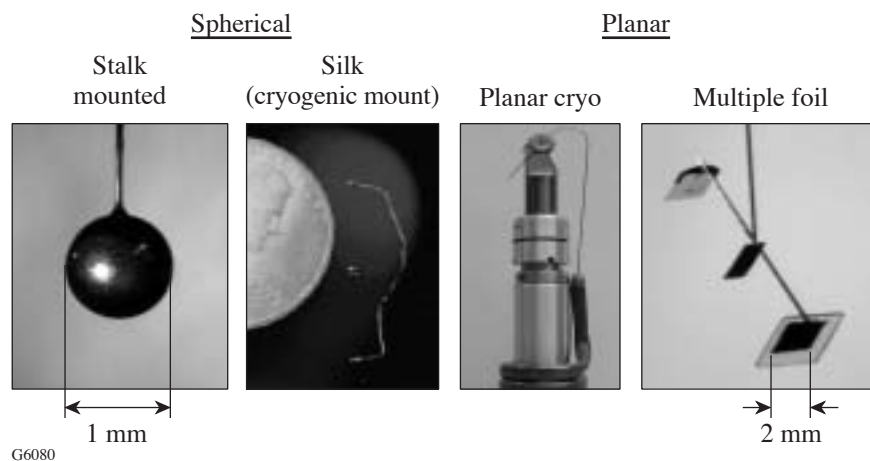


Figure 2.1-1
From left to right: Stalk-mounted coated target, silk-mounted cryogenic target, planar-cryo target, multiple-foil target.

2.1.1 Glass and Polymer

Current spherical implosion targets, such as those shown in Fig. 2.1-2, consist of thin-walled glass or plastic shells filled with a DT or DD gas mixture that may contain trace amounts of a diagnostic gas. Depending on the type of experiment, these targets are coated with various metals, inorganic (salt), and polymeric materials (see Fig. 2.1-2). Target-quality glass and plastic shells are fabricated by General Atomics, the DOE-designated target contractor and supplier for the ICF fusion community. The desired gas mixture is permeated into the shell at room temperature if the shell material is plastic or at $\sim 300^{\circ}\text{C}$ if the material is glass. The required soak times are determined from the measured permeation time constant for each gas and the shell-wall properties.

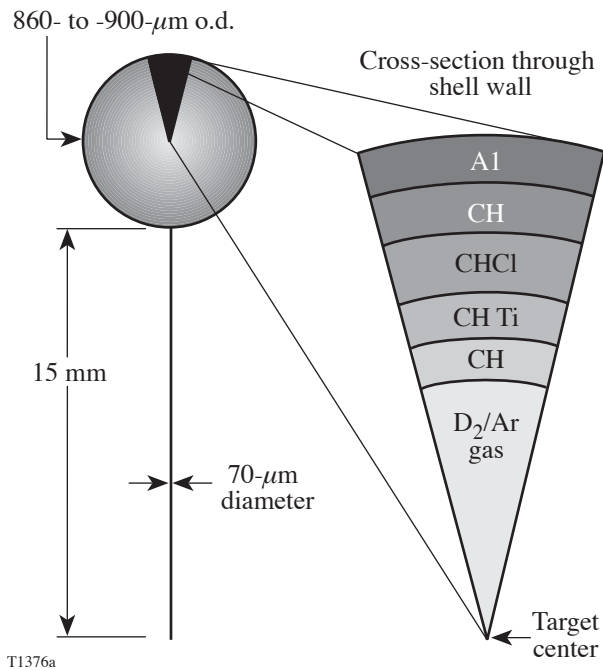


Figure 2.1-2
Typical spherical target dimensions with example of layer types.

Spherical polymer capsules are typically $\sim 870\ \mu\text{m}$ in diameter and with wall thicknesses varying from 2 to 30 μm , depending upon the goal of the experiment. While polymer shells are desirable for their low density, mass, and atomic weight, they are more complex and expensive to produce than glass shells. The best surface smoothness is $\sim 60\text{-nm}$ rms roughness for $2 \leq \ell \leq 100$, although typical smoothness values are ~ 40 to 200 nm.

Plastic targets are available with a discrete layer of plastic doped with a mid- to high-atomic-weight element at a well-defined location in the shell wall. Elements such as silicon, germanium, chlorine, and titanium are available at concentrations of 6%, 2%, 3%, and 5%, respectively. The actual concentration is known to $\pm 20\%$ of the requested dopant level.

A variation of the partially doped target is the “surrogate” cryogenic target. Here, the hydrogen in the plastic is replaced with either deuterium or a combination of deuterium and tritium. Fully deuterated plastic shells are available. Mid- z “spectroscopic marker” atoms may be present at discrete regions of the capsule wall.

The polymer shells are filled with D_2 or DT to pressures of 2 to 40 atm. Trace concentrations of inert gases, i.e., Ne, Ar, Kr, and Xe, can be added to the D_2 (only) gas. All non-cryogenic shells are coated with 500 Å to 700 Å of Al on the outside of the shell as a shinethrough and permeation barrier.

2.1.2 Foam Targets

A new type of plastic shell under development is the foam shell (Fig. 2.1-3). The shell wall is 50 to 100 μm thick and consists of a resorcinol-formaldehyde (RF) open-cell foam with a density of 80 to 180 mg/cm^3 . A 2- to 4- μm GDP overcoat is vapor deposited over the foam to seal the shell. These targets are filled with D_2 for ICF experiments.

The first OMEGA cryogenic wetted-foam target implosion produced the highest neutron yield to date.

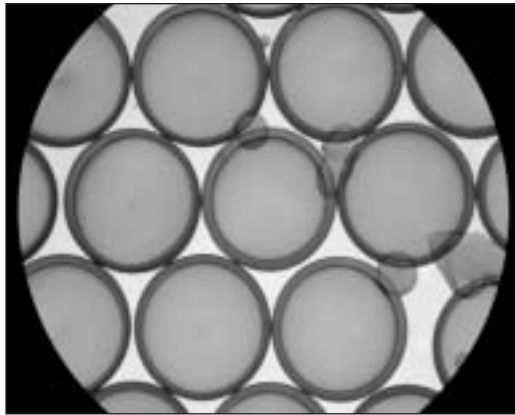


Figure 2.1-3
R/F foam targets in liquid.

11404

2.1.3 Coatings

The application of coatings to targets is a necessary step in the fabrication of many of the multilayered shells required by different experiments. Several processing systems are available: Deposition methods such as thermal evaporation and sputtering (physical vapor deposition) are used to provide metallic coatings. Plastic coatings (e.g., CH) are applied by the vapor phase deposition of oligomers that polymerize on the surface. A parylene generator is available for plastic deposition. Salt coatings, such as KBr, KCl, NaF, and NaCl, are deposited using evaporation techniques.

Uncoated glass shells are essentially impermeable to hydrogen at room temperature. Bare plastic shells, on the other hand, are highly permeable and must be coated with a thin layer of aluminum prior to filling. The aluminum layer extends the permeation time constant from about 2 min to 6 to 10 h. This allows the desired gas mixture to be established and maintained through subsequent processing. After the initial coating step, the gas mixture is permeated into the shell over a 24- to 48-h period. When permeation is complete, it may be necessary to add an additional 900-Å layer of aluminum. This final layer seals the target and acts as a shinethrough barrier. This technique has been used to fill polymer shells with D_2 , DT, and mixtures of up to three gases: Ne, Ar, Kr, and Xe, each of which has a different permeation rate. To ensure that the target contains the required, known amount of gas, the completed targets are delivered to OMEGA in individual pressurized capsules and are depressurized just prior to being inserted into the target chamber.

2.1.4 Surface Finish

The smoothness of the outer and inner capsule surfaces is important. The shells must be spherical (to within $<0.5\%$ of the radius) and the walls concentric. The rms surface roughness, calculated from the power spectrum of the modes, is desired to be less than 80 nm for modes $\ell = 2-100$. Both GA and LLE use a modified atomic force microscope (AFM) to profile surface roughness along discrete great circles around a target. (The target is mounted on an air bearing and rotated beneath the AFM sensing head. The circularity and alignment of the target are sufficient to ensure that the target surface remains within the dynamic range of the AFM.)

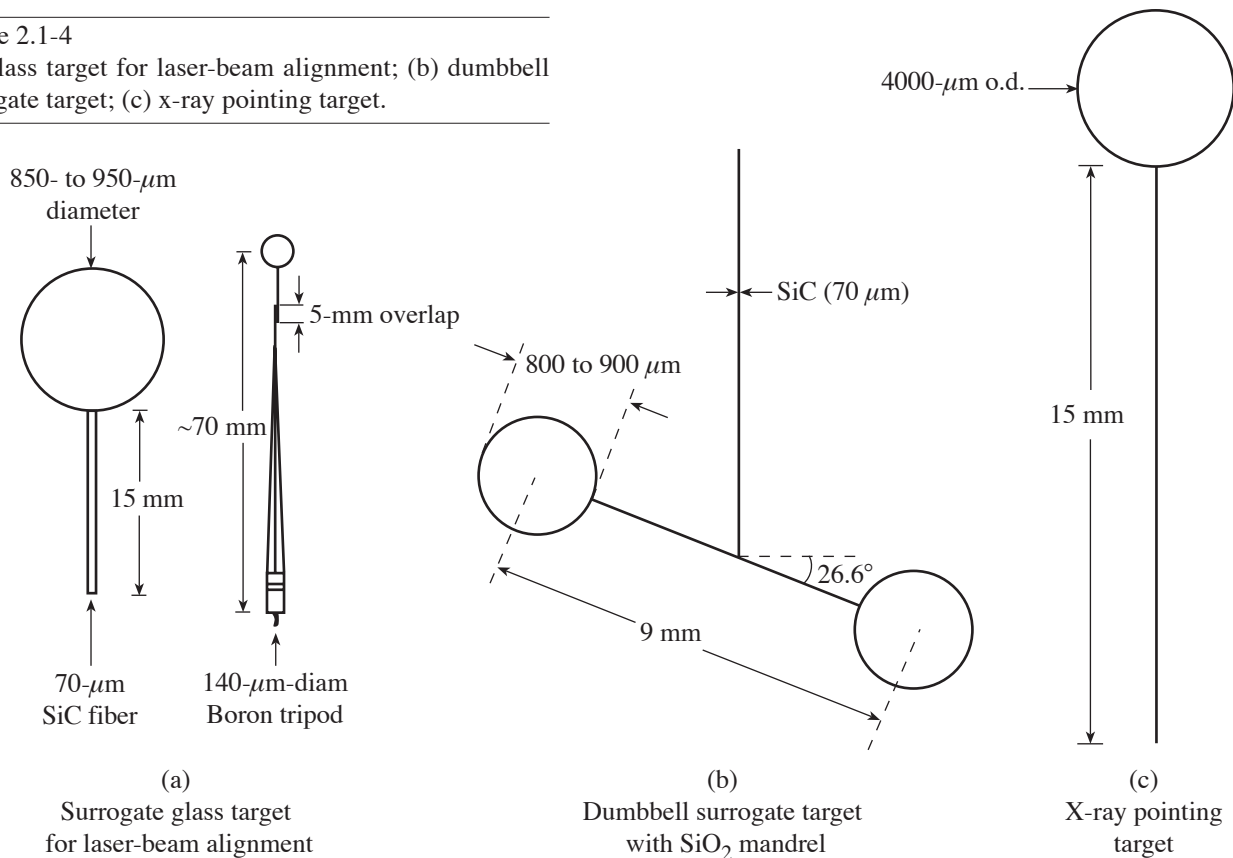
2.1.5 Low-Mass Target Mounts

The technique used to support the target is important for the following reasons: (1) the mass in contact with the target must be kept to a minimum to avoid perturbing the physics of the experiment; (2) the total amount of material in the mount must be minimized to limit damage to optics and diagnostics inside the target chamber due to material ablated from the mount; (3) the mount must not occlude any of the 60 beams; and (4) target vibration must be kept below the level required by the experiment. In addition, the mounts for cryogenic targets must be stable and durable at cryogenic temperatures (16.8 K).

Some typical current target mounts are shown in Fig. 2.1-4. For routine target-mounting requirements, a 15-mm-long, $17\text{-}\mu\text{m}$ -diam SiC fiber is attached to the target. This, in turn, is attached to a 1-cm-long, $70\text{-}\mu\text{m}$ -diam SiC fiber and then to a 7-mm, $140\text{-}\mu\text{m}$ boron fiber. Finally, a boron-fiber

Figure 2.1-4

(a) Glass target for laser-beam alignment; (b) dumbbell surrogate target; (c) x-ray pointing target.



tripod supports the carbon fiber. This mount assembly has caused no ablation damage and has a resonant frequency >200 Hz, which is high enough for this application. (The resonant frequency is routinely measured prior to delivering targets.)

The “C-mount” design has been developed to support cryogenic targets. Here the target is suspended by spider’s silk between the open ends of a C-shaped mount fabricated from beryllium. For alignment reasons, the target must be positioned within $50\ \mu\text{m}$ of a centroid position defined by the C mount and the cryogenic equipment.

2.2 CAPSULES FOR CRYOGENIC TARGETS

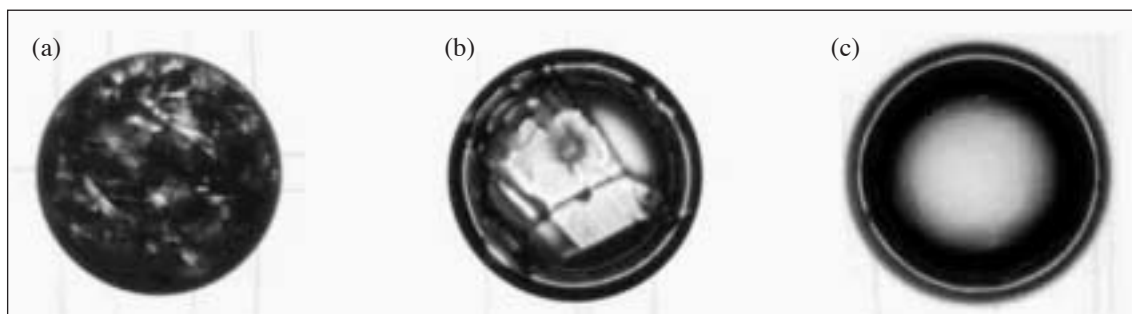
OMEGA cryogenic capsules make use of a thin (a few microns thick) glow discharge plasma (GDP) or polyimide shell that contains the fusion fuel. A typical target design for the OMEGA laser system consists of a spherical shell, $0.9\ \text{mm}$ in diameter and 1 to $5\ \mu\text{m}$ in wall thickness (see Fig. 2.2-1), with a $100\text{-}\mu\text{m}$ -thick layer of solid deuterium and tritium (DT) uniformly deposited on the inner surface.

Figure 2.2-2 shows, from left to right, (a) an “unlayered” plastic target containing frozen deuterium and (b) a partially layered target. Note the crystalline faceting between the ice crystals. The bright ring is the inner surface of the ice shell. Image (c) shows a well-layered target. The hallmark of



S258

Figure 2.2-1
GDP target.



G6069

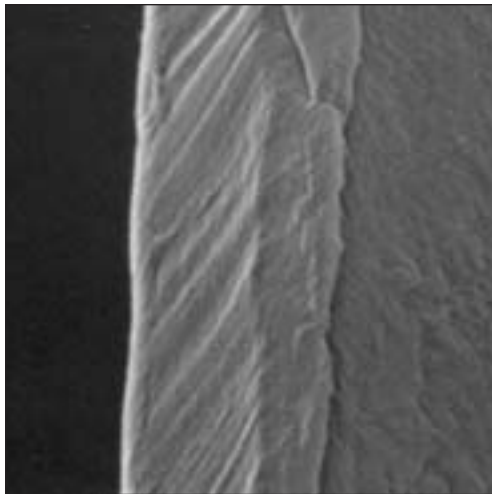
Figure 2.2-2
Layering of a cryogenic target.

a well-layered target is the uniform radius of the bright band and the absence of crystal bounding facets. On each image the faint black lines are spider webs. These webs are used to attach the target to the C-shaped holder or mount.

2.2.1 Polyimide and Glow Discharge Polymer (GDP) Fabrication

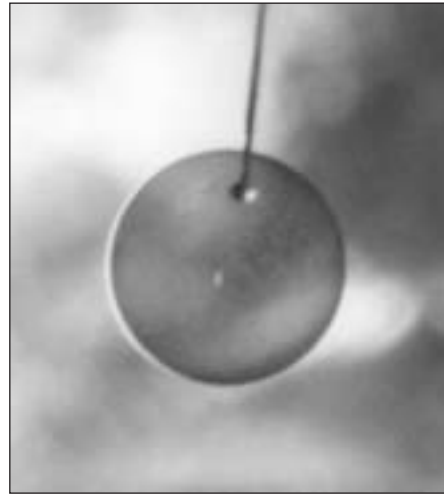
Polyimide is an optimum material for ICF targets because it has high tensile strength, high Young's modulus, and great resistance to radiation. This increases the survivability rate for thin-walled shells. The standard shell material at LLE is GDP because it has lower density and better (smoother) surface roughness, and the production process is more developed.

Polyimide and GDP shells can be consistently fabricated with dimensions (see Figs. 2.2-3 and 2.2-4) required for ICF targets. The properties and quality of shells can be modified and improved via processing parameters. The modifications in the shell properties are attributed to changes in crystallinity and the degree of cross-linking.



T1436a

Figure 2.2-3
Cross section through the polyimide capsule
showing the wall.



T1436b

Figure 2.2-4
Polyimide capsule.

Spherical polyimide shells are fabricated using a vapor-deposition polymerization (VDP) method. In this work, a parametric study was performed to optimize the fabrication process and quantify the associated properties relevant to cryogenic targets.

The polyimide fabrication deposition process involves two steps. PMDA and ODA are vapor deposited to form poly (amicacid) (PAA) on either PAMS mandrels or flat substrates. The PAA layer is then converted into polyimide by thermal imidization. In this process, the PAMS mandrel is depolymerized and permeated out of the nascent polyimide layer, resulting in freestanding shells. Figure 2.2-5 shows the process, and Fig. 2.2-6 shows the chemical synthesis.

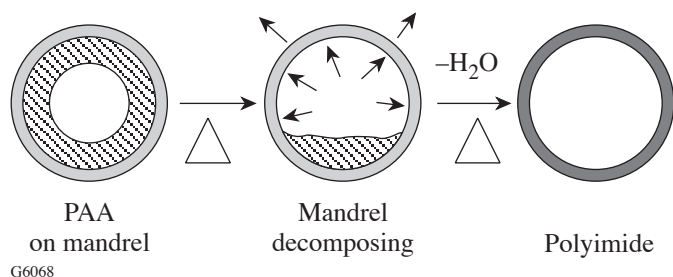


Figure 2.2-5
Polyimide fabrication deposition process.

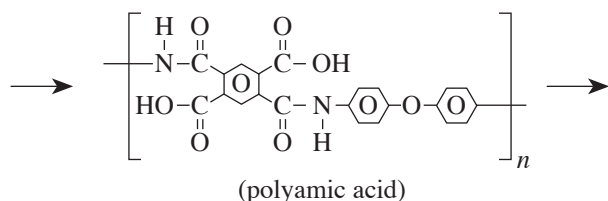
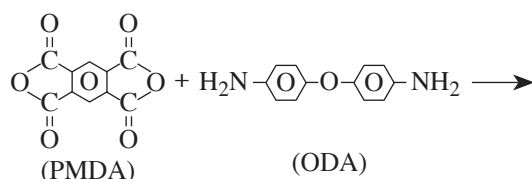
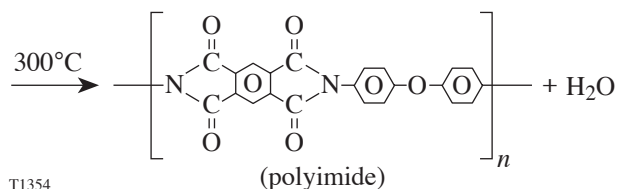


Figure 2.2-6
Polyimide chemical synthesis.



T1354

The glow discharge polymer (GDP) process is simpler. Two source gases— C_3H_6 (or acetylene) and hydrogen—pass into a glow discharge, which causes the carbon-based gas to polymerize on the mandrel.

The depolymerizable mandrel technique was recently developed by GA and LLNL to fabricate plastic ICF targets. The mandrels were either solid beads or hollow shells made from poly(*a*-methylstyrene) (PAMS) that were overcoated with GDP using the traditional low-pressure glow discharge polymerization process.

Heating the overcoated mandrel to 300°C decomposes the mandrel into its individual monomer units that permeate through the shell wall.

Currently, the PAMS mandrels are thin-walled ($<10\text{-}\mu\text{m}$) shells (0.85- to 0.95-mm diam) fabricated by the microencapsulation method. This method was initially developed to make polystyrene shells for ICF experiments but is better suited for making mandrels. This process meets the critical requirement of the mandrel, which is a smooth, spherical surface.

2.2.1.1 Target Burst and Buckle Parameters

The elastic modulus and tensile strength of both polyimide and GDP shells must be known to define the conditions required to prepare DT-filled cryogenic targets: (1) the greater the elastic modulus, the greater the buckling pressure the target can withstand, and (2) the greater the tensile strength, the greater the burst pressure the target can endure. These values and the permeability of the material determine the maximum rate at which the target can be pressurized and cooled for ICF cryogenic experiments.

LLE's burst and buckle test equipment consists of a pressure cell with opposing windows, a microscope, a CCD camera, and a pressure transducer with an accuracy of ± 1 psi. The shells are viewed through a microscope with transmitted light. The shell's image, the gas pressure in the cell, and the elapsed time are all recorded on videotape.

To burst (or buckle) a shell, the pressure in the chamber is lowered (or raised) at a faster rate than the rate that the internal shell pressure changed due to permeation through the shell wall (Fig. 2.2-7 shows a target that has buckled under 5 atm of overpressure). Typical pressure-rate changes ranged from 0.01 atm/s to 3.5 atm/s for buckle tests and up to 50 atm/s for burst tests. After the shell fails, the videotape is reviewed frame-by-frame to determine the exact rupture pressure. If the permeation time constant of the shell is known, the pressure difference across the shell wall at the point of failure can be accurately calculated, and the strength measurement is corrected for this change. The sequence of images shown in Fig. 2.2-8 shows a burst test of a target; the capsule is seen to swell prior to bursting.



Figure 2.2-7
Target buckled due to external overpressure of 5 atm.

2.2.1.2 Permeability

The rate at which hydrogen isotopes permeate through the plastic material is a major factor that will determine the viability of vapor-deposited capsules as target-shell material. A high room-temperature permeation rate will allow targets to be rapidly filled to the designated pressure (maximum is 1500 atm) for cryogenic ICF experiments. A slow room-temperature permeation rate will require that the targets be filled at elevated temperatures (200°C max); otherwise the material cannot be used. It is necessary that the material be impermeable below 26 K and desirable, although unlikely, that the material be permeable above ~ 50 K. This latter capability will prevent a pressure differential from developing across the shell wall during the cooling cycle (due to temperature gradients in the permeation vessel).

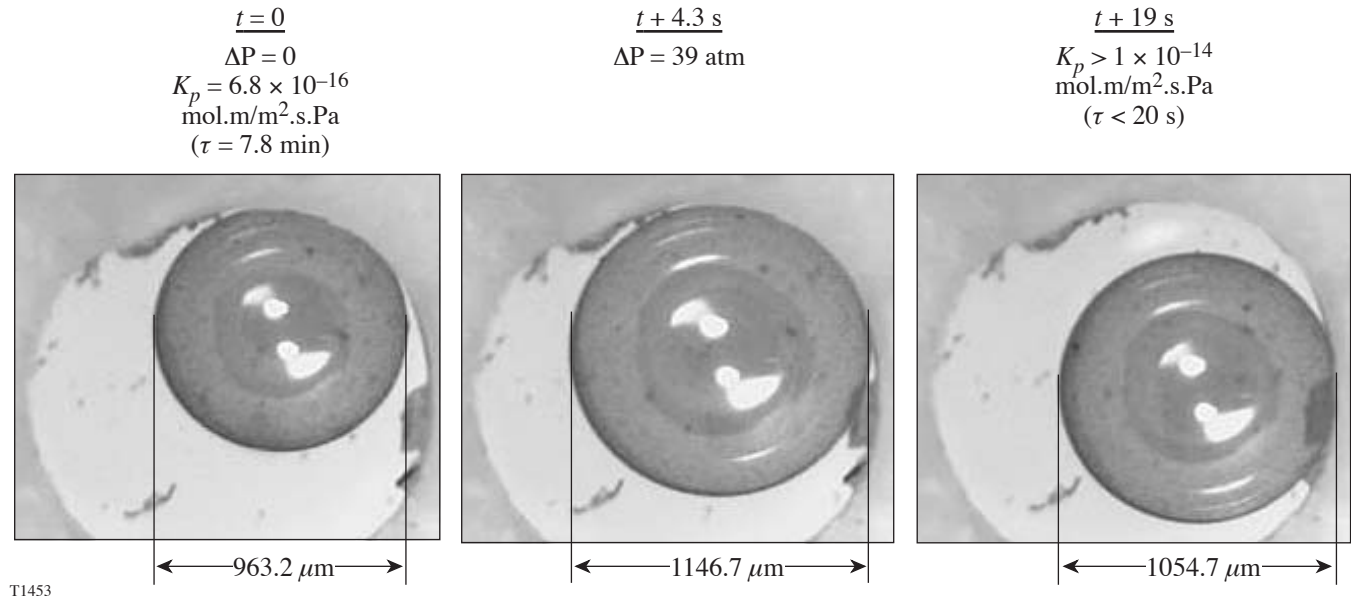


Figure 2.2-8

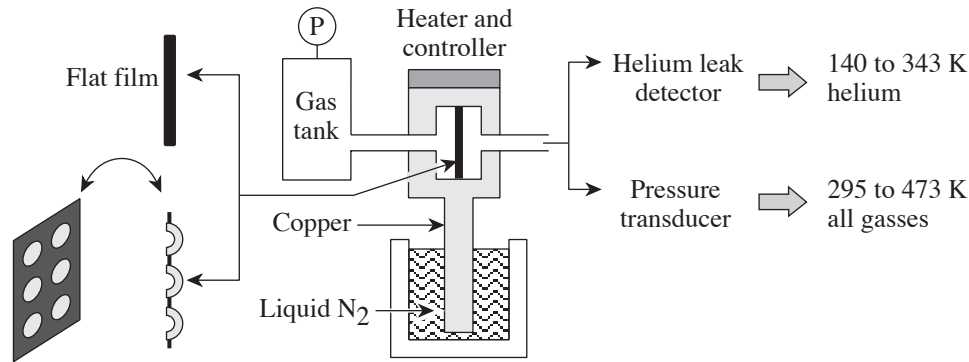
A 39-atm pressure differential across a polyimide capsule (with a 5- μm wall) increases the capsule diameter by 19%, the surface area by 42%, and the permeability by more than 100%.

The permeability of a shell is measured by permeating gas into the shell and then transferring it into a (pre-baked) chamber of known volume (2.4 cm³). The pressure rise in the chamber is monitored as a function of time, and the data are fitted with the expected exponential function. A correction term is added to this function to account for outgassing from the chamber walls ($\sim 4 \times 10^{-11}$ Torr•l/cm²•s). The equation gives the shell's permeation time constant (for the specific gas) and the total quantity of gas in the shell at the time the pressure measurement begins.

To determine the effect of temperature on the permeability of the shell material, the technique is modified as illustrated in Fig. 2.2-9. Half-shells are mounted on a metal plate and placed into a chamber of known volume. One side of the plate is pressurized via a gas tank; the other side of the plate has a pressure transducer and He leak detector. The permeability rate is measured as the temperature is varied from 140 K to 473 K.

The technique allows permeation time constants as short as 1 min and as long as 50 h to be measured with accuracy greater than 95%. The permeation time constant t is determined from the plot of pressure rise versus time.

The material permeability coefficient K_p is determined using the permeation time constant of a thin spherical container, $t - 1 = (K_p ARgT) / wV$, where A is the shell's mean surface area, Rg is the ideal gas constant, T is the absolute temperature, w is the shell's wall thickness, and V is the shell volume. For a thin-walled spherical shell this simplifies to $K wr RTpg = 3t$, where r is the average shell radius.



Half-shells
mounted
on metal plate
T1667

Figure 2.2-9
Experiment that measures temperature dependency of
the plastic permeation from 140 K to 473 K.

2.3 TARGET MOUNTING

A rugged low-mass mount, shown in Fig. 2.3-1, has been developed that satisfies the numerous requirements. Spider-silk fibers as thin as $0.25 \mu\text{m}$ are readily available in essentially any length. Four fibers are stretched across the arms of a convoluted beryllium wire ($250\text{-}\mu\text{m}$ diam), and the capsule is inserted between them in a precise and repeatable location. The capsule is glued to the fibers.

The Be frame is attached to a boron fiber, which in turn is attached to an Al base [see Fig. 2.3-2(a)]. This mounting method is highly robust at cryogenic temperatures. The wire frame is convoluted so that it is compatible with the present OMEGA 60-beam configuration, causing minimal disruption to the beam path. In addition, the support structure must not occlude the diagnostic ports. A modified frame without the convolutions (needed to avoid blocking the beams) is also used.

The four targets are placed in a contoured copper holder, as shown in Fig. 2.3-2(b). The copper holder acts to improve the temperature uniformity inside the permeation cell and also provides a space filler to minimize the volume [see Fig. 2.3-2(b)]. Four targets are filled simultaneously.

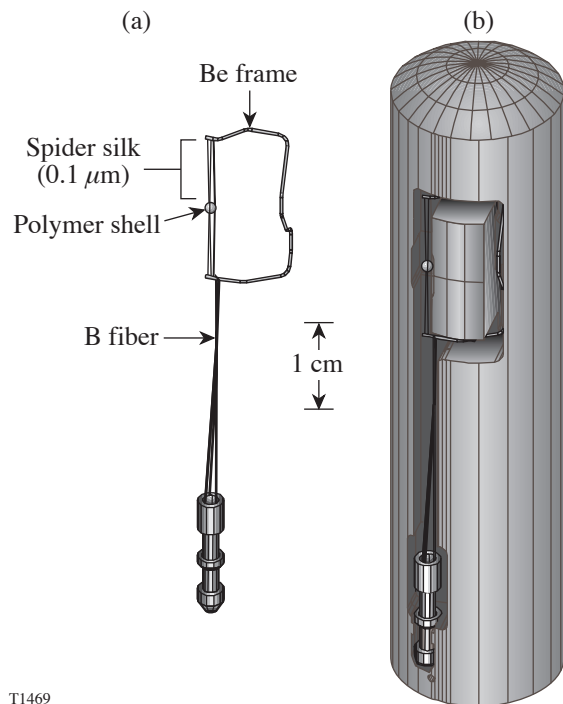
The specifications for the mounting structure are the following:

- Cannot occlude laser beams
- Cannot occlude diagnostic ports
- Rigid support of the capsule
- Resonant vibration frequency about the target positioning system
- Must achieve stiffness with fibers longer than 3 mm
- Must consist of materials of low atomic numbers that can survive the cryogenic temperatures without distortion
- Must not absorb a significant amount of DT during permeation



T1639

Figure 2.3-1
Spherical target mounted on a convoluted Be frame with four spider silks.



T1469

Figure 2.3-2
(a) A silk-mounted polymer shell on a Be frame, which is attached to a boron fiber; (b) the target rack showing a mounted target inserted in one of four slots.

2.3.1 Spider Silk

Spider silk has proven to be the optimum material for mounting targets in the beryllium frame (see Fig. 2.3-3).

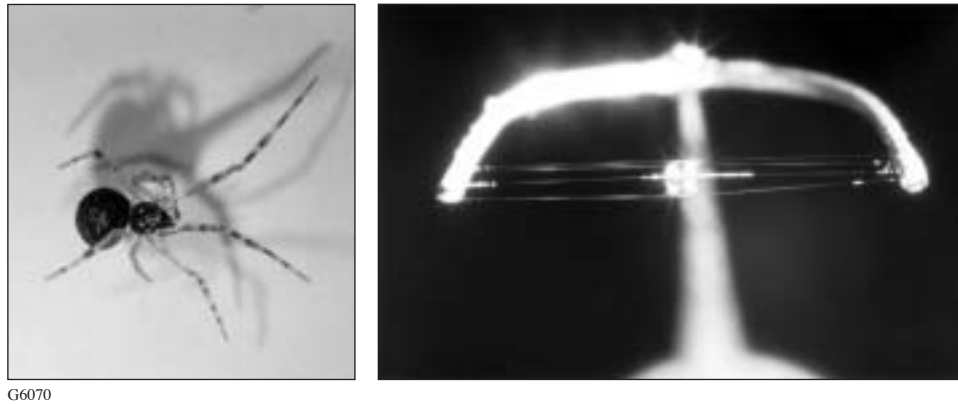


Figure 2.3-3
Spider and silk-mounted target.

2.3.2 Spider-Silk Tensile Strength

One strand of spider silk will support a 16-mg target, which is 300 times the mass of cryo targets.

The spider silk has desirable tensile strength properties as can be seen in Fig. 2.3-4. The average ultimate tensile strength for silk is 1.2 GPa (see Fig. 2.3-5). A 50- μ g cryogenic (filled) target exerts a load of 0.2 MPa, which is negligible compared to the tensile strength of the silk. To minimize vibration, the silk is preloaded to about 800 MPa (16% strain). The stress-strain behavior of the spider silk (see Fig. 2.3-5) is typical of the silk from spiders obtained locally.

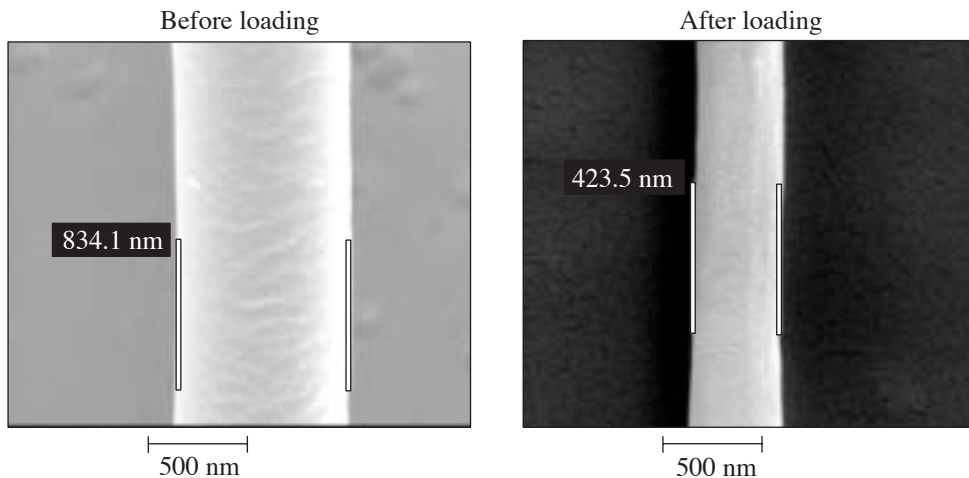


Figure 2.3-4
SEM images of spider silk
before and after loading.

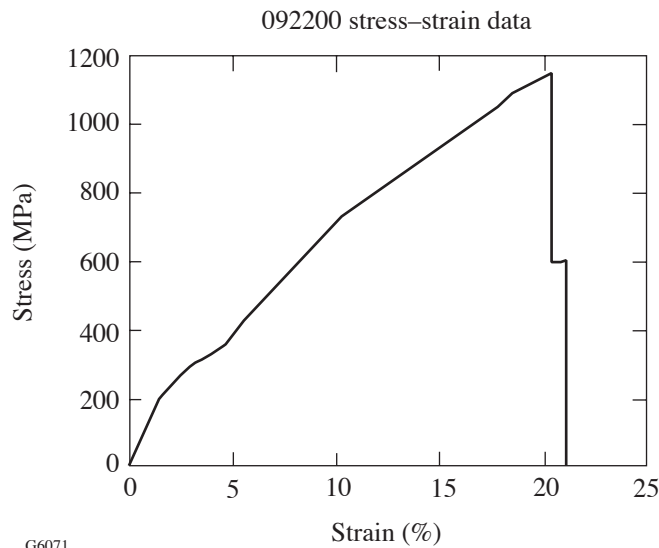


Figure 2.3-5

Typical stress-strain data. The maximum strain is 20%. Notice that after the silk ruptures, the data plateau at 600 MPa. This indicates that two parallel silk strands were loaded.

2.3.3 Mechanical Properties of Silk

The characterization of spider silk produces the following average values with a 95% confidence level:

- Elastic modulus 2.2 ± 0.7 GPa
- Ultimate tensile strength 1.2 ± 0.2 GPa
- Elongation 25%
- Energy to break $1.4 \pm 0.3 \times 10^5$ J/kg

2.4 PLANAR CRYOGENIC TARGETS

A representative planar-target cell structure used for equation-of-state experiments is shown in Fig. 2.4-1. The fill gas condenses and freezes in the cell. Windows and internal components can be changed to suit the experimental requirements. Beryllium windows can be provided for transverse x-ray imaging.

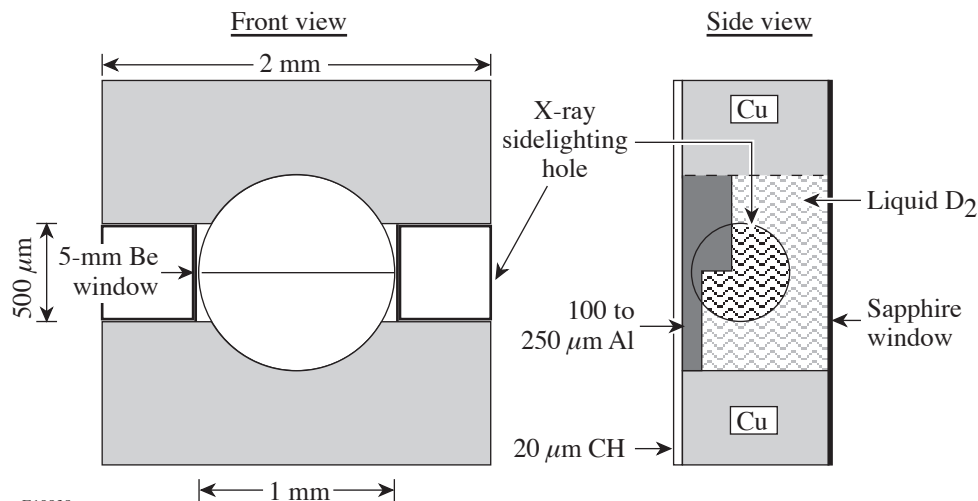


Figure 2.4-1

Cryogenic-planar-target cell structure used for equation-of-state experiments.

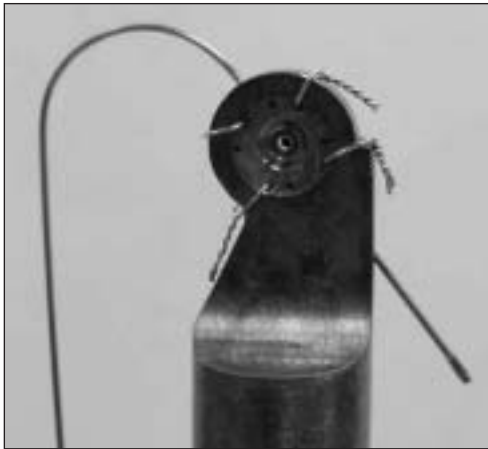
Each target cell is composed of numerous small components that must be meticulously cleaned, assembled, and thoroughly tested (see Figs. 2.4-2, 2.4-3, 2.4-4, and 2.4-5).

The MC is inserted into the OMEGA chamber from the bottom. Approximately 1.5 s prior to a shot, the shroud is rapidly removed from the MC to expose the target. Figure 2.4-6 shows a planar target shot. The target cell is destroyed during the shot (see Fig. 2.4-7). The target holder and reservoir can be recovered and reused. The active shock breakout (ASBO) diagnostic (ten o'clock) is used to measure the velocity of laser-induced shock waves that propagate through the target cell.



G6072

Figure 2.4-2
Planar targets are carefully assembled by hand.



G6073

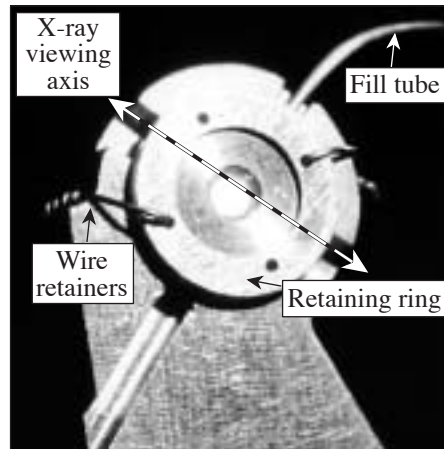
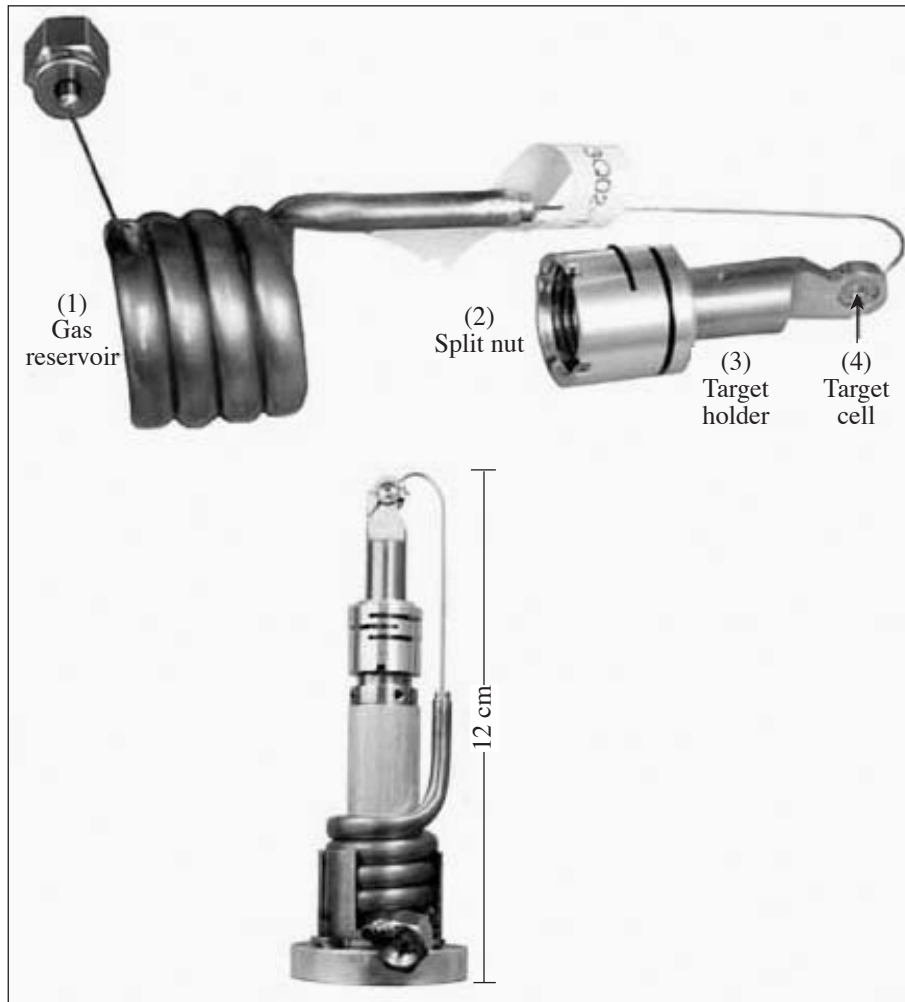


Figure 2.4-3

A close-up view of the target assembly. The target cell is clamped between a pair of retaining rings that prevent hardware from being ejected into the OMEGA chamber. Slots machined at one and seven o'clock are for the fill and vent tubes. Slots machined at four and ten o'clock are provided for transverse x-ray imaging.



G6074

Figure 2.4-4

A planar cryogenic target assembly ready for filling. The coiled copper reservoir (1) is filled with room-temperature gas (e.g., D_2) before attaching the target assembly to the cold head. The target holder (3) is secured to the cold head with the split nut (2), providing conductive thermal coupling.



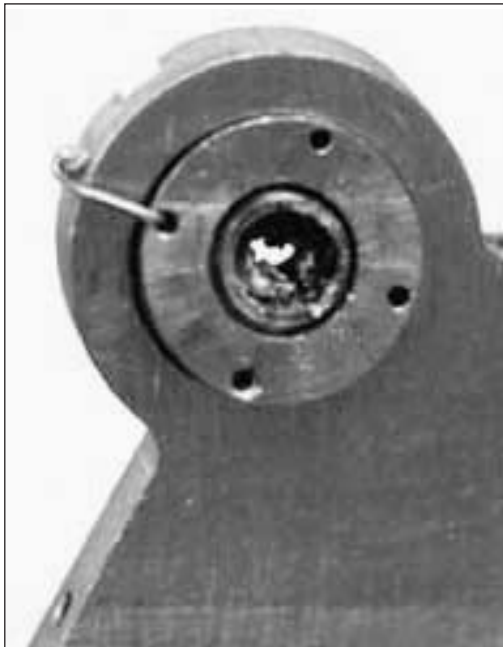
Figure 2.4-5
Fully assembled cryogenic planar target.

G6075



G5570

Figure 2.4-6
A photograph of a cryogenic planar shot
inside the OMEGA chamber.



G6076

Figure 2.4-7
The target shot destroys the target cell.

2.5 QUALITY ASSURANCE

The Powell scope metrology station is the primary diagnostic used to measure the dimensional accuracy of an assembled target (see Fig. 2.5-1).

The permeability of the aluminum overcoat used to contain the fill gas in a capsule for room-temperature implosions is measured using the permeator time-constant apparatus. The runout is measured by rotating the target about a pin axis (see Fig. 2.5-2).



T1594

Figure 2.5-1
The Powell scope metrology station. This provides 4° of motion to manipulate the target's position and orthogonal camera views to measure dimensions.



T1589

Figure 2.5-2
The runout must be kept to a minimum.

2.5.1 Silk and Mount Resonance

The high elastic modules and significant preload result in a high resonant frequency for low-magnitude impulse-driven signals. The resonant frequency of a “C-mounted” target was measured to be 142 Hz when driven by a piezoelectric transducer and function generator operating at 2.5-V amplitude (see Fig. 2.5-3). The GDP target weighed 69 μg with an 877- μm OD and a 30- μm wall thickness. Three strands of silk were used in this configuration. Table 2.5-1 contains results from this test configuration.

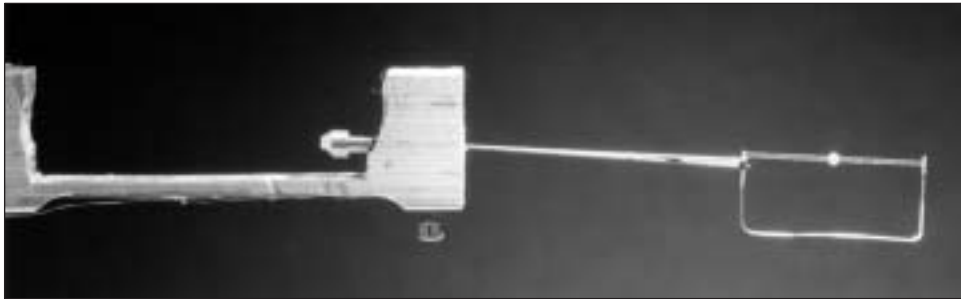


Figure 2.5-3
Piezoelectric transducer
cryogenic target resonator.

T1595

Table 2.5-1: Mounted target resonant frequency as measured by the piezoelectric transducer.

Average Outer Diameter (μm)	Average Wall Thickness (μm)	Shell Material	Average Resonant Frequency (Hz)	Standard Deviation (Hz)
925	3.4	CH, CD	297	26
938	9.1	CD	272	39
935	10.0	CD	322	13
932	25.7	CH	260	39